Holocene coastal reconstruction, Naikoon peninsula, Queen Charlotte Islands, British Columbia

S.A. Wolfe, I.J. Walker, and D.J. Huntley

2008

Geological Survey of Canada
Current Research 2008-12

Natural Resources Canada
Ressources naturelles Canada

Canada

ISSN 1701-4387
Catalogue No. M44-2008/12E-PDF
ISBN 978-0-662-48864-4

A copy of this publication is also available for reference in depository libraries across Canada through access to the Depository Services Program's Web site at http://dsp-psd.pwgsc.gc.ca

A free digital download of this publication is available from GeoPub:
http://geopub.nrcan.gc.ca/index_e.php

Toll-free (Canada and U.S.A.): 1-888-252-4301

Recommended citation

Wolfe, S.A., Walker, I.J., and Huntley, D.J., 2008. Holocene coastal reconstruction, Naikoon peninsula, Queen Charlotte Islands, British Columbia; Geological Survey of Canada, Current Research 2008-12, 16 p.

Critical reviewer
B. Vaughn

Authors

S.A. Wolfe (swolfe@nrcan.gc.ca)
Geological Survey of Canada
601 Booth Street
Ottawa, Ontario K1A 0E8

I.J. Walker (ijwalker@uvic.ca)
Department of Geography
University of Victoria
P.O. Box 3050
Victoria, British Columbia V8W 3P5

D.J. Huntley (huntley@sfu.ca)
Department of Physics
Simon Fraser University
8888 University Drive
Burnaby, British Columbia V5A 1S6

Correction date:

Holocene coastal reconstruction, Naikoon peninsula, Queen Charlotte Islands, British Columbia

S.A. Wolfe, I.J. Walker, and D.J. Huntley

Wolfe, S.A., Walker, I.J., and Huntley, D.J., 2008. Holocene coastal reconstruction, Naikoon peninsula, Queen Charlotte Islands, British Columbia; Geological Survey of Canada, Current Research 2008-12, 16 p.

Abstract: The Holocene coastal landscape of northeastern Graham Island, British Columbia is reconstructed from ca. 9.5 ka to present based on surficial geology and geomorphic mapping using light detection and ranging techniques, high-resolution aerial photographs and ground truthing, and dating of coastal deposits using optical and radiocarbon dating methods. Six evolutionary phases are defined over the Holocene. A predominantly erosional shoreline, initially featuring steep, bluff-backed shorelines and river inlets, evolved into an increasingly depositional coastal landscape with raised marine terraces, a northward-extending spit complex, and prograding lowland foredune and beach ridge systems. The modern system hosts an eroding shoreline backed by landward-migrating parabolic dunes and foredunes with localized erosional bluffs.

Shoreline reconstructions indicate a Holocene marine highstand of about 15.5 m a.m.s.l. at ca. 9.5 ka. By 5 ka, a deep embayment, acting as a depositional sink, was formed when Tow Hill joined the mainland which, in turn, initiated rapid progradation of North Beach. Since about 2.7 ka, rapid and possibly accelerating rates of beach ridge and foredune progradation have occurred, coupled with extension of the Rose Spit complex. During this period, the 'East beach' shoreline eroded, removing evidence of past shorelines and older geomorphic features. Nearshore sediment transport has occurred along both North Beach and East beach coupled with high eolian activity. West of Tow Hill, geoarcheological evidence dating to ca. 3.1 ka from atop a high bluff promontory may indicate a possible Haida occupation site at that time. Beach progradation has also occurred along this section of shoreline in the last 3.0 ka, with Yakan Point becoming attached to the mainland by about 1.2 ka.

Résumé : Le paysage côtier holocène de la partie nord-est de l'île Graham, en Colombie-Britannique, a été reconstitué pour la période d'environ 9,5 ka jusqu'au présent d'après la géologie de surface et la cartographie géomorphologique, à l'aide de méthodes de détection et de télémétrie par la lumière, de photographies aériennes à haute résolution et de vérifications au sol, et par la datation des dépôts côtiers par des méthodes optiques et au radiocarbone. Six phases d'évolution ont été définies pour l'Holocène. Un littoral formé principalement par érosion, présentant à l'origine des rivages et des embouchures de cours d'eau donnant contre des escarpements, a évolué vers un littoral caractérisé par une sédimentation croissante et comportant des terrasses marines soulevées, un réseau de flèches littorales allongées vers le nord et des réseaux progradants d'avant-dunes et de crêtes de plage de faible altitude. La zone côtière actuelle présente un rivage en érosion à l'avant d'avant-dunes et de dunes paraboliques qui migrent vers l'intérieur des terres, ainsi que, par endroits, des escarpements érodés.

Les reconstitutions du littoral indiquent qu'un haut niveau marin holocène d'environ 15,5 m au-dessus du niveau moyen de la mer, prévalait il y a environ 9,5 ka. Déjà il y a 5 ka, une baie profonde qui jouait le rôle de bassin de sédimentation s'était formée par suite du fusionnement de la colline Tow au continent, ce qui a ensuite provoqué une progradation rapide de la plage North. Depuis environ 2,7 ka, il y a progradation rapide, voire même accélérée, des crêtes de plage et des avant-dunes et prolongement du réseau de la flèche Rose. Pendant cette période, l'érosion du rivage de la « plage East » a fait disparaître les vestiges de rivages antérieurs et d'entités géomorphologiques plus anciennes. Le transport des sédiments littoraux le long des plages North et East s'est combiné à une activité éolienne marquée. À l'ouest de la colline Tow, des indices géoarchéologiques remontant à environ 3,1 ka au sommet d'un haut promontoire d'un escarpement, donnent à penser que les Haïdas ont occupé le site à cette époque. Il y a également eu progradation de la plage le long de cette partie du littoral depuis 3,0 ka, et la pointe Yakan s'est fusionnée au continent il y a environ 1,2 ka.

INTRODUCTION

Global climate changes are affecting the world's coastal communities, many of which are vulnerable to ongoing climatic variability impacts (Intergovernmental Panel on Climate Change, 2007). Given geologically rapid rates of relative sea-level change and the extensive area and potential magnitude of these impacts, coastal vulnerability assessments have received significant international attention. In Canada, climate change affects coastal communities through gradual effects of sea-level rise, and more immediate risks of extreme events including increased storm-surge flooding, accelerated coastal erosion, tidal encroachment, contamination of coastal aquifers, and various ecological changes. Canada has the longest coastline in the world, about one-third of which has a moderate to high physical sensitivity to sea-level–rise impacts (Shaw et al., 1998). Nevertheless, until recently, very little research had been conducted on coastal zone impacts and community adaptations to climate change, particularly in British Columbia (e.g. Walker and Sidneysmith, 2008).

The impacts of climate change and sea-level rise are of particular concern in British Columbia's coastal communities which, in addition to physical impacts, have seen significant economic restructuring in the wake of fishing and forestry declines in the past 25 years (Dolan and Walker, 2006; Ommer, 2007; Walker and Sidneysmith, 2008). This study is part of a larger case study that examined the coastal vulnerability to climate change and sea-level rise on northeast Graham Island (Queen Charlotte Islands), British Columbia (Dolan and Walker, 2006; Walker and Barrie, 2006; Walker et al., 2007). The overall objective of the case study was to investigate the environmental and social impacts of climatic change and accelerated sea-level rise on one of Canada's most sensitive coastal regions and, from this, assess adaptive capacity. The purpose of this component of the study was to establish a geological context, including an understanding of coastal geomorphic responses to past sea-level changes during the Holocene. The objectives were to map the surficial geology of the northeastern 'Naikoon peninsula' (informal name), and accurately date and reconstruct Holocene shoreline positions and geomorphic features formed during the latest Holocene sea-level regression.

STUDY AREA

The study area is the northeastern portion of Graham Island, the largest island in the Queen Charlotte Islands archipelago (Fig. 1). The area, known as the Naikoon peninsula, lies within the wet hyper-maritime subzone of the Coastal Western Hemlock Biogeoclimatic Zone. Much of the inland area consists of raised bogs interspersed with wetland forest containing a ground cover of mosses, lichens, liverworts, herbs, and shrubs. Inland of the long, dune-backed sandy shorelines are distinctive forest communities dominated by

Figure 1. Naikoon peninsula of northeastern Graham Island, Queen Charlotte Islands, with satellite image depicting study area.

Sitka spruce (*Picea sitchensis*), shore pine (*Pinus contorta*), Western Redcedar (*Thuja plicata*), and various herbaceous species including large-headed sedge (*Carex macrocephala*), dune grass (*Leymus mollis*), and Pacific alkali grass (*Puccinellia nutkaensis*). This climate and ecology provides for rapid colonization and stabilization of backshore landforms.

The Queen Charlotte Islands has a history of human occupation extending for at least the last 10 000 years (Fedje and Mackie, 2005). During this time, the Haida have maintained close ties with the sea, living alongside it and benefiting from its resources. Numerous places of cultural, spiritual, and ecological significance, including prehistorical Haida village sites such as Tao (Tow Hill) and Nai-kun ('House point' (informal name) or Rose Spit) occur throughout the Naikoon area and figure prominently in traditional Haida origin stories. The modern name, 'Naikoon', is a corruption of the Haida term, Nai-kun, or long nose, referring to Rose Spit, which extends off the northeastern tip of Graham Island (Fig. 1). According to Haida legends, some of the oldest villages stood along the eastern shore of Naikoon peninsula. Prehistorical villages were also found at the mouth of the Hiellen and Oeanda rivers. An archeological site dating to about 3.3 ka BP also occurs at Tow Hill (Severs, 1975), though very few detailed archeological investigations have occurred in the Naikoon peninsula study area (described in

Mackie and Acheson (2005) and Fedje and Mackie (2005)). (The terms 'ka BP' and 'a BP' designate uncalibrated radiocarbon ages, whereas 'cal ka BP' and 'cal a BP' designate calibrated radiocarbon ages (prior to AD 1950); 'ka' and 'a' used herein on their own designate ages derived from optical dating (prior to AD 2004)'.

Colonial settlement of Queen Charlotte Islands began in the mid- to late 1800s, encouraged by early coal-mining interests and subsequent free Crown Grants (Dalzell, 1968). Early settlers drained wetlands on the Naikoon peninsula for farming and cattle pastures. The majority of these ventures failed, with only a few settlers remaining after the 1930s. Evidence of past settlement activities such as wagon roads, drainage ditches, pastures, and river diversions are still visible today, as are remnants of placer mining and forestry. In 1973, the Provincial Government designated the Naikoon peninsula area as a Class A Provincial Park covering an area of about 72 000 ha (Fig. 1) lying entirely within the Queen Charlotte Lowland Ecoregion. A number of early settlement lots were subsumed and still remain as privately owned lands, wholly contained within Naikoon Provincial Park.

Today, the Naikoon peninsula represents an important cultural and natural resource for the Haida and other local residents. For instance, North Beach has an important Haida commercial fishery for razor clams and Dungeness crabs. Seasonal deer hunting is also a popular food-gathering exploit for locals. The park is a popular tourist destination for camping, hiking, all-terrain vehicle use, and beachcombing, and hosts three campgrounds. Some homes, seasonal cottages, and backcountry shacks have been built along the northern and, to a much lesser extent, eastern shorelines within the park.

This area is identified by the Geological Survey of Canada as in the top 3% of Canada's most sensitive coasts to accelerated sea-level–rise impacts (Shaw et al., 1998). The moderate to high sensitivity of this coastline is due to a macrotidal range, erodible sediments, frequent windstorms and surges, and an energetic wave climate that produce a dynamic coast where some areas are eroding at 1–3 m/a to tens of metres in extreme seasons such as the 1997–1998 El Niño event (Barrie and Conway, 1996, 2002). Consequently, this coast is highly vulnerable to ongoing regional sea-level rise (1.6 mm/a), and to extreme water-level events related to climatic variability, which are rising at more than twice the rate of the regional sea-level rise (3.4 mm/a; Abeysirigunawardena and Walker (in press)).

Numerous traditional Haida stories reveal knowledge of changing sea levels entrenched within their culture (Fedje et al., 1996; Wilson and Harris, 2005). Indeed, the late Quaternary sea-level history of the British Columbia west coast is one of the most dynamic in North America. Regional sea levels on the northern Pacific margin of Canada fell dramatically after the late Wisconsin glacial maximum. Crustal flexure and rebound caused by a glacio-isostatic forebulge initiated rapid sea level regression ca. 14.6–12.4 cal ka BP to 150 m below present sea level in southern Hecate Strait (Josenhans et al., 1997), and to as much as 100 m below present sea level in northern Hecate Strait (Barrie and Conway, 1999, 2002; Hetherington et al., 2003). At that time, much of Hecate Strait east of the Naikoon peninsula was subaerially exposed and may have provided a corridor for early human migration (Josenhans et al., 1995).

After ca. 14 cal ka BP, eustatic sea-level rise and subsidence of the forebulge caused rapid sea-level transgression, as fast as 50 mm/a (Clague et al., 1982a, Josenhans et al., 1995, 1997), to a highstand at about 15–16 m by ca. 8000–9000 a BP (9–10 cal ka BP) on northeastern Graham Island (Clague et al., 1982a; Clague, 1989) and similarly, at about +14 to 16 m by ca. 9000 a BP (10.1 cal ka BP) in the southern Queen Charlotte Islands. Evidence of this transgression occurs offshore as drowned shorelines, river channels, estuaries, deltas, spits, barrier islands, and wave-cut terraces (e.g. Warner et al., 1982; Josenhans et al., 1995, 1997; Barrie and Conway, 2002), as well as submerged archeological sites and artifacts (e.g. Fedje and Josenhans, 2000). After the highstand, sea level fell at approximately 2.0 mm/a (Clague et al., 1982a).

The northeastern tip of the Naikoon peninsula retains a surficial geological record of the latest Holocene sea-level regression in the form of relict beach ridges, stabilized foredunes, prograding spits, and extensive stabilized parabolic dune systems (Barrie and Conway, 2002; Walker and Barrie, 2006). The purpose of this study is to map the surficial geology of the northeastern Naikoon peninsula, and to accurately date and reconstruct Holocene shoreline positions and geomorphic features formed during the latest Holocene sea-level regression.

METHODS

LiDAR and surficial mapping

High-resolution airborne LiDAR (light detection and ranging) data and coincident digital orthophotographs (at 25 cm resolution) were flown in July and September, 2006. The LiDAR data were flown at approximately 1300 m at a pulse rate of 50 kHz (scanned at 30 Hz in Z-scan pattern) along 1 km swaths. This yielded a ground coverage density of 0.6–2.0 points/m^2 with a vertical accuracy of 10–30 cm (depending on ground-cover type). Elevation data were georeferenced to UTM 09 map projection and the NAD 83 horizontal datum corrected to mean sea level (m.s.l.) using the Canada 2000 Geoid HT 2.0 model. From this, a digital elevation model, relative to mean sea level was compiled by the Hyperspectral-LiDAR Research Group in the Department of Geography, University of Victoria. In addition, a combined digital photomosaic, draped on the bare earth DEM (digital elevation model) was created; a portion of which is shown in Figure 2a.

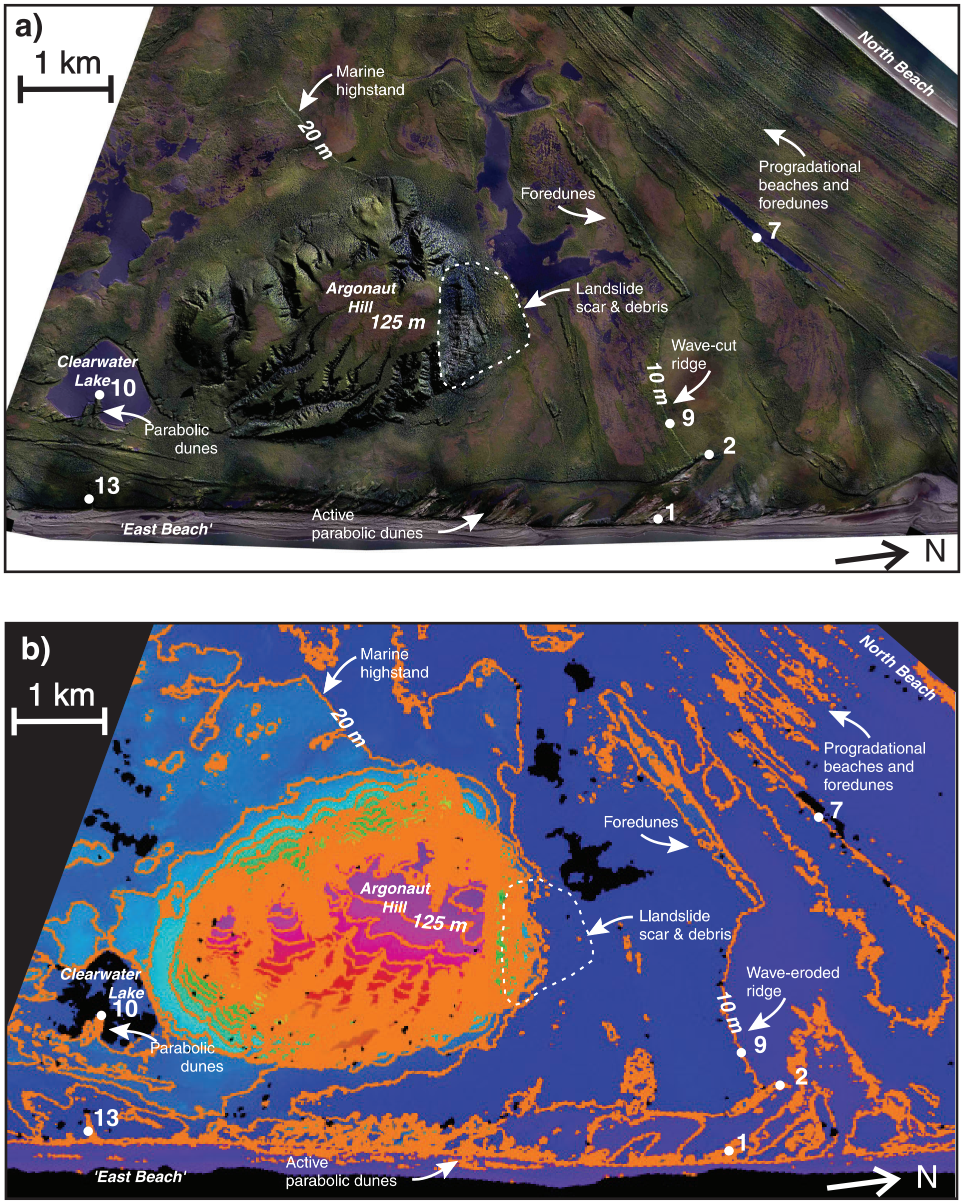

Figure 2. Example of LiDAR and high-resolution orthophotographic imagery for part of study area shown in Figure 1. **a)** High-resolution orthophotographic imagery draped over DEM created from LiDAR, highlighting various geomorphic features. **b)** Elevation map with 5 m contour spacing and location of some sample sites in Table 1.

The digital photomosaic DEM, combined with older monochromatic airphotos were used to interpret surficial geology and geomorphic features (e.g. dune ridges, former shorelines), identify and locate sampling locations for optical dating, and reconstruct phases of coastal evolution. Field ground truthing and sample collection was conducted during four field campaigns between spring 2003 and 2005.

Optical and radiocarbon dating chronology

To determine former relative shoreline positions and elevations, several optical dating sample sites were selected strategically from airphotos. Nine samples were dated from distinctive backshore landforms, including former foredunes and parabolic dunes, and one sample from an active blowout was dated for zero-age determination (Table 1). Samples from stabilized features were collected from pits or exposed sections to avoid potential mixing of the parent dune sand with overlying pedogenically altered sediments. Test pits were deepened to approximately 1.5 m and samples were taken from 1–1.2 m depth in eolian sand, sampled in the dark, and stored in a sealed container. Eolian stratigraphy was verified at each sample site by noting pedogenic development, bedding structures, and occurrence of buried soils or other materials. Pits were infilled and georeferenced in the field to within 10–20 m positional accuracy (NAD 83) using handheld GPS units. Locations and sample elevations were more accurately determined afterward using LiDAR data.

Optical dating measures the time elapsed since mineral grains were last exposed to sunlight, which may correspond to the time since the grains were buried. Optical dating techniques are described elsewhere (e.g. Wintle, 1997; Aitken, 1998; Huntley and Lian, 1999; Lian and

Table 1. Optical age and accelerator mass spectrometry radiocarbon sample locations.

Site no.	Sample no. (field ID)	Latitude (N)	Longitude (W)	Sample elevation (m a.m.s.l.)	RSL (m)[a]	Feature	Dated material
1	SFU-O-284 (SAW03-02)	54°04'17.97"	131°40'36.46"	5.1	0.0	Modern blowout	Eolian sand
2	SFU-O-285 (SAW03-03)	54°04'30.42"	131°41'10.92"	10.5	0.0	Stabilized parabolic dune	Eolian sand
3	SFU-O-286 (SAW03-04)	53°59'29.65"	131°42'06.27"	5.0	<1.0	Modern wave-cut ridge, mid-section	Eolian sand
4	SFU-O-283 (SAW03-01)	53°59'31.16"	131°42'21.11"	24.7	<1.0	Stabilized parabolic dune	Eolian sand
5	SFU-O-291 (SAW04-02)	54°07'22.02"	131°41'20.12"	7.2	<2.0	Stabilized foredune	Eolian sand
6	SFU-O-292 (SAW04-03)	54°07'09.00"	131°40'49.01"	8.2	<3.0	Stabilized foredune	Eolian sand
7	SFU-O-288 (SAW03-21)	54°05'01.92"	131°42'53.15"	15.0	<4.5	Stabilized foredune	Eolian sand
8	SFU-O-290 (SAW04-01)	54°01'22.08"	131°58'31.14"	44.0	<15.5	Eolian sand on wave-cut ridge	Eolian sand
9	SFU-O-287 (SAW03-20)	54°04'20.40"	131°41'24.92"	11.5	<8.5	Eolian sand on wave-cut ridge	Eolian sand
10	SFU-O-289 (SAW03-22)	54°01'19.12"	131°42'32.31"	26.0	<14.0	Stabilized parabolic dune	Eolian sand
11	WDA04-03A	54°06'19.68"	131°40'03.58"	-0.5	<2.0	Marine clay	Pine cone
12	WDA04-03B	54°06'19.68"	131°40'03.58"	-0.5	<2.0	Marine clay	Seaweed
13	WDA04-01A	54°01'11.39"	131°41'37.33"	12.0	<8.0	Terrestrial material over marine deposits	Peat, stems, roots
14	WDA04-08	54°01'22.08"	131°58'31.14"	44.0	<15.5	Eolian sand on wave-cut ridge	Peat, stems
15	WDA04-04B	54°01'22.88"	131°58'31.20"	28.0	<15.5	Wave-cut ridge, mid-section	Peat, plant fragments

[a] RSL (relative sea level) is the approximate former sea-level position relative to present mean sea level.

Huntley, 2001) and Lian et al. (2002) provide methodological details applied to this study. Sand-sized (180–250 μm diameter) K-feldspar grains were dated by excitation with near-infrared (1.4 eV, ~880 nm) photons and measuring the violet (3.1 eV, 400 nm) photons emitted in response. The multiple-aliquot additive-dose with thermal transfer correction method was used to determine the equivalent dose. This dose, together with a measure of the environmental dose rate and a correction for anomalous fading, was used to calculate the ages (Table 2, 3). This technique has been used successfully on sand dunes in the Canadian Great Plains (Wolfe et al., 2004), with ages that are in agreement with radiocarbon ages (Wolfe et al., 2002) and an optical age derived from quartz (Huntley and Lamothe, 2001).

Radiocarbon dating was conducted on terrestrial and marine plant materials at the University of California Ervine KECK Carbon Cycle AMS Facility. All samples were subjected to a standard acid-base-acid treatment. Multiple AMS (accelerator mass spectrometry) ages were determined on each sample in order to assess appropriateness of the materials for dating. Two samples of uniform organic materials (site 11, pine cone; site 12, seaweed; Table 4) were collected within clayey sediments exposed in the intertidal zone near Fife Point (Fig. 1). Other samples, containing peat, degraded organic material, plant stems, and roots were collected from terrestrial sites, at depths ranging from the surface to about 80 cm. In these settings, the introduction of younger and modern organic material (via roots and organic accumulation) poses a potential problem to dating. Therefore, ages were determined on subsets of samples that were carefully separated into different organic material types. Even so, the ages used from these terrestrial sites should be considered minimums, due to the possible incorporation of younger organic materials. Radiocarbon ages were calibrated to calendar years using Calib 5.0.1 (Stuiver et al., 2005) with the calibration data set of Reimer et al. (2004).

Table 2. Potassium, thorium, and uranium concentrations used for dosimetry, and water contents of samples.

Site no.	Lab number	Depth (cm)[a]	K (% ± 5%) Sample	K (% ± 5%) Surroundings[b]	Th (μg/g) ± 0.1	U (μg/g) ± 0.1	Water content[c]
1	SFU-O-284	0	1.04	0.97	5.2	2.03	0.01
2	SFU-O-285	100	1.15	1.11	7.0	1.40	0.07
3	SFU-O-286	100	1.10	1.21	2.7	0.97	0.10
4	SFU-O-283	340	1.09	1.05	6.9	1.63	0.07
5	SFU-O-291	100	0.81	0.85	10.1	2.17	0.08
6	SFU-O-292	100	0.98	0.94	5.2	1.17	0.14
7	SFU-O-288	100	1.20	1.12	2.7	1.11	0.15
8	SFU-O-290	60	1.05	1.03	3.3	1.39	0.23
9	SFU-O-287	100	1.10	1.09	3.4	1.11	0.17
10	SFU-O-289	90	1.22	1.21	2.2	0.72	0.20

[a] Sample depth beneath the ground surface, and used for calculation of the cosmic-ray dose rate. For SFU-O-283 the depth was 40 cm except for the past 60 years (determined from tree rings of buried spruce trees, during which it was 340 cm).
[b] Average of K content of samples collected 30 cm below and above the main sample.
[c] Water content = (mass water)/(dry mineral mass), based on as-collected values (average of three samples) and used for long-term estimates.
Note: Rb contents were in the range of 15-40 μg/g.

Table 3. Total dose rate, equivalent doses (De), and optical ages with 1σ uncertainties.

Site no.	SFU Lab. #	$\dot{D}$ (Gy/ka)[a]	D_e (Gy)	Uncorrected optical age[b] (ka)	Fading rate[c] (%/decade)	Delay[d] (days)	Corrected optical age[e] (ka)
1	SFU-O-284	3.24 ± 0.08	0.06 ± 0.15	0.02 ± 0.05	5.4 ± 0.6	35	-----
2	SFU-O-285	3.09 ± 0.08	-0.03 ± 0.10	-0.01 ± 0.03	-----	36	-----
3	SFU-O-286	2.65 ± 0.08	0.41 ± 0.08	0.15 ± 0.03	-----	36	0.18 ± 0.04
4	SFU-O-283	3.09 ± 0.08	0.87 ± 0.10	0.28 ± 0.03	-----	35	0.34 ± 0.04
5	SFU-O-291	3.12 ± 0.11	1.43 ± 0.13	0.46 ± 0.05	-----	115	0.55 ± 0.06
6	SFU-O-292	2.70 ± 0.12	2.64 ± 0.35	0.98 ± 0.14	-----	115	1.2 ± 0.2
7	SFU-O-288	2.68 ± 0.08	5.20 ± 0.2	2.02 ± 0.10	-----	20	2.7 ± 0.2
8	SFU-O-290	2.63 ± 0.13	6.40 ± 0.7	2.43 ± 0.29	-----	101	3.1 ± 0.4
9	SFU-O-287	2.63 ± 0.08	10.2 ± 0.6	3.88 ± 0.26	4.9 ± 0.9	20	5.2 ± 0.4
10	SFU-O-289	2.54 ± 0.08	11.7 ± 0.9	4.80 ± 0.39	5.5 ± 0.5	21	6.5 ± 0.6

[a] Total dose rate is the sum of α, β, γ, and cosmic-ray contributions.
[b] Optical ages, *not* corrected for anomalous fading.
[c] Fading parameters calculated from data between 1.6 days and 4 months or more after laboratory irradiation, as described for method 'b' in Huntley and Lamothe (2001). The larger uncertainty for #287 is due to interaliquot variability for this sample. A decade is a factor of ten in time since irradiation.
[d] Delay is the time between laboratory irradiation and equivalent dose measurements
[e] Optical ages, corrected for anomalous fading using the delay time listed and a fading parameter of 5.4 ± 0.5%/decade for all.
Notes: Aliquots used for thermal transfer correction were given a daylight bleach.
----- not calculated.

Table 4. Accelerator mass spectrometry radiocarbon samples and ages.

Site no.	Sample #	UCIAMS Lab #	Material	Sample depth (cm)	$\delta^{13}C$	Age (a BP; $\pm 1\sigma$)	Age range (cal a BP ; $\pm 1\sigma$)[a]	Age range used (cal a BP)
11	WDA04-3A	10143 10529	Pine cone	0–5	-26.8 -24.1	1350 ± 25 1330 ± 20	1298–1276 1291–1268	1298–1268
12	WDA04-3B	10144 10530	Seaweed fragments	0–5	-10.7 -13.4	2000 ± 25 1970 ± 20	1598 –1519[b] 1563 –1490[b]	1598–1490
13	WDA04-1A	10528	Peat (bulk matrix)	0–5	-28.8	3240 ± 30	3479–3403	3479–2979
		10142 10150	Bulk peat		-25.0 -39.4	3095 ± 35 2890 ± 20	3367–3265 3365–2979	
		10372 10527	Plant stems or roots		-27.2 -28.7	2585 ± 25 2405 ± 20	2748–2726 2457–2355	-----
14	WDA04-08	10374	Silty peat and degraded organic material	75–80	-23.7	2955 ± 25	3201–3077	3201–3077
		10147 10533	Plant stems or roots		-30.5 -29.0	-420 ± 20 -880 ± 30	Modern	-----
15	WDA04-4B	10148	Charred plant fragments	Surface	-21.9	3025 ± 30	3322–3169	3322–3169
		10151 10373 10532	Peat with charred plant fragments		-23.6 -21.4 -22.0	2760 ± 25 1965 ± 20 2145 ± 20	2915–2794 1931–1884 2292–2072	-----

[a] Radiocarbon ages calibrated using Calib 5.0.1
[b] Radiocarbon date calibrated using 100% marine option in Calib. 5.0.1.
----- not used.

RESULTS

Surficial geology and geomorphology

Figures 2a and b illustrate some of the geomorphic features and elevations observed in the study area as interpreted from the LiDAR DEM and colour orthophotographs. The 20 m elevation contour delineates a wave-cut ridge marking the upper limit of the Holocene marine highstand. The actual highstand elevation, as defined by the average elevation of the base of the wave-cut ridge at several locations, is 18.5 m a.m.s.l. The most prominent feature in Figure 2 is Argonaut Hill, rising more than 100 m above the surrounding peninsula. On the northern end of Argonaut Hill is a large landslide scar and debris flow that appears to have occurred subsequent to the marine highstand, as there is no apparent wave-cutting of the landslide scar or debris. At lower elevations, numerous nearshore and backshore features occur including wave-eroded beach ridges, stabilized foredunes and parabolic dunes, progradational ridges, and active parabolic dunes (Fig. 2a, b).

Figure 3a depicts the surficial geology and geomorphology of northern Naikoon peninsula, as interpreted from airphoto and LiDAR data and ground truthing, with dated sites and chronological control. The legend for Figures 3a–f describes the features and sediments for these maps. Bedrock outcrops include Late Tertiary sandstone and shale of the Skonun Formation and Late Pliocene or Early Oligicene basalt of the Tow Hill sills (Sutherland Brown, 1968). Late Wisconsin sediments and landforms include extensive glacial meltwater-derived fluvial outwash plains, and discrete interfluve remnants as represented by Argonaut Hill and Eagle Hill. Holocene surficial features and sediments residing below the Holocene marine highstand include colluvial deposits, estuarine sediments, and a suite of nearshore and terrestrial coastal deposits represented by marine erosional and depositional terraces, sand dunes (active and stabilized), spits, and beaches.

Tow Hill and Yakan Point represent the only bedrock outcrops in the study area (Fig. 3a). Late Tertiary sandstone and shale of the Skokun Formation outcrop at both sites (Sutherland Brown, 1968). At Tow Hill, they are intruded by younger, Late Pliocene or Early Pleistocene olivine columnar basalt of the Tow Hill sills, which rise up to about 100 m a.m.s.l. Inland, at elevations above about 18.5 m a.m.s.l. (i.e. above the Holocene marine highstand), are unconsolidated late-glacial and Quaternary sediments. Most of the surficial terrain above the marine highstand consists of sandy, glacial meltwater-derived outwash sediments. Although the hummocky surface over most of the plain may indicate deposition over stagnant ice (Clague et al., 1982b), the area is thought to have resided beyond the extent of ice sheets during the late Quaternary glacial maximum (Sutherland Brown, 1968; Warner et al., 1982). Argonaut Hill, Eagle Hill, and other un-named uplands to the south are remnants of thicker glacial outwash sediments that were not eroded during later glaciofluvial incisions. Argonaut Hill is comprised largely of unconsolidated, crossbedded outwash sand and silt. Exposures in excess of 50 m height reveal massive deposits of crossbedded silty sand.

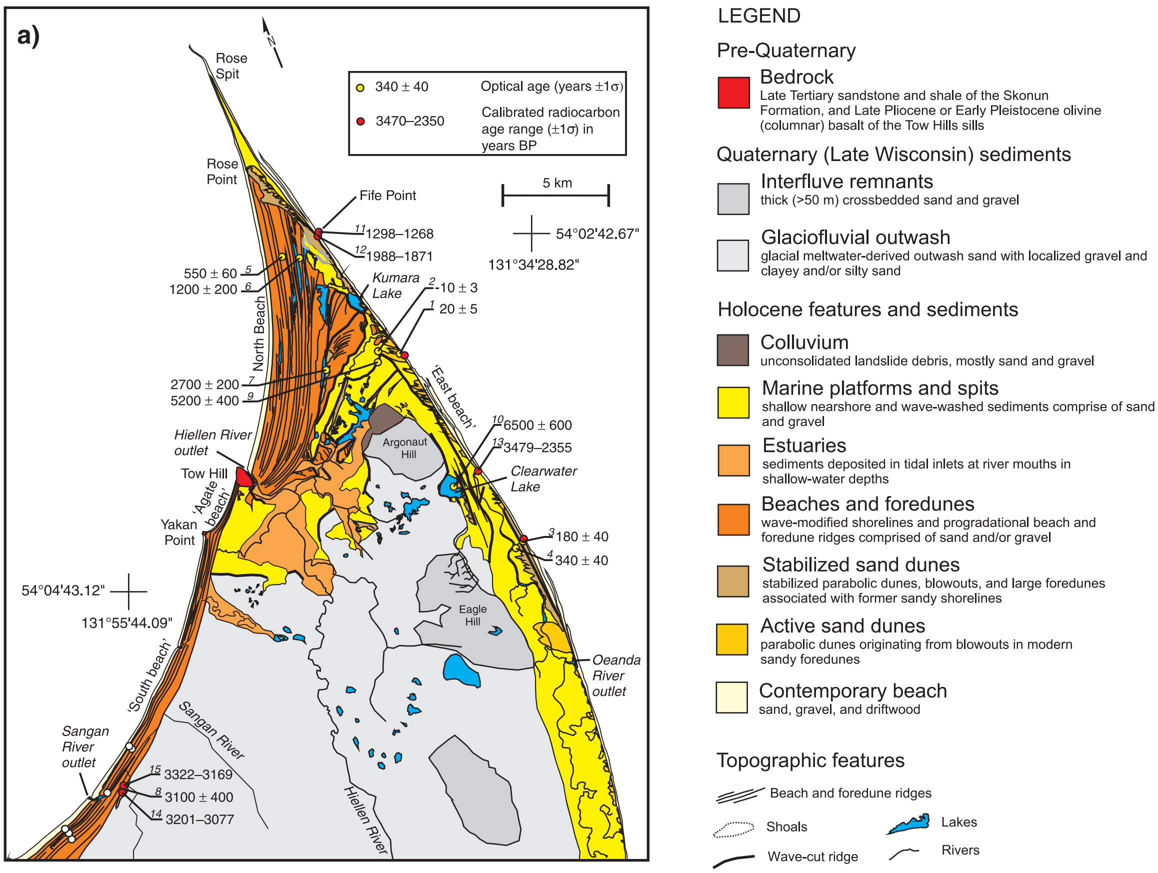

Figure 3. a) Present-day surficial geology and geomorphology of study area with optical and radiocarbon dating control.

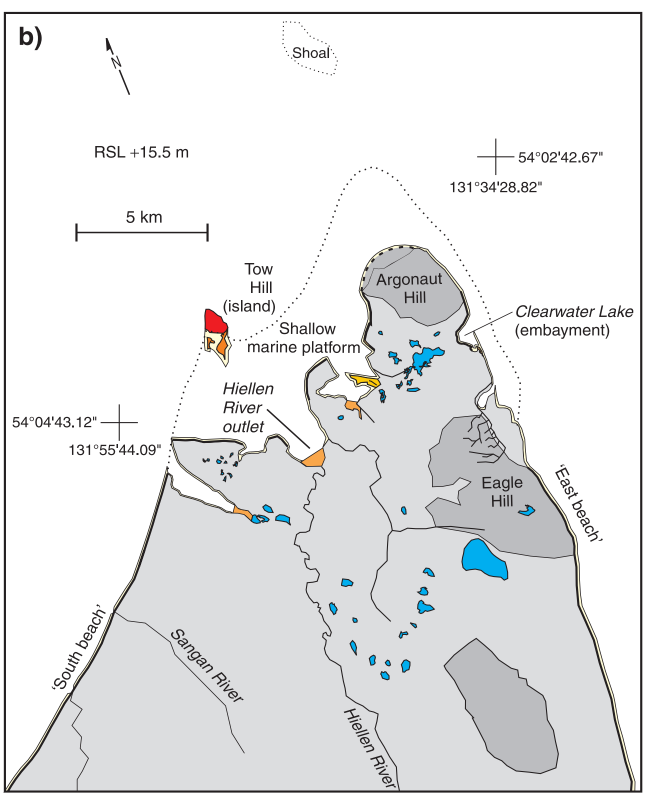

Figure 3. b) Interpreted shoreline position, surficial geology, and geomorphology for ca. 9.5 ka, with relevant dating control.

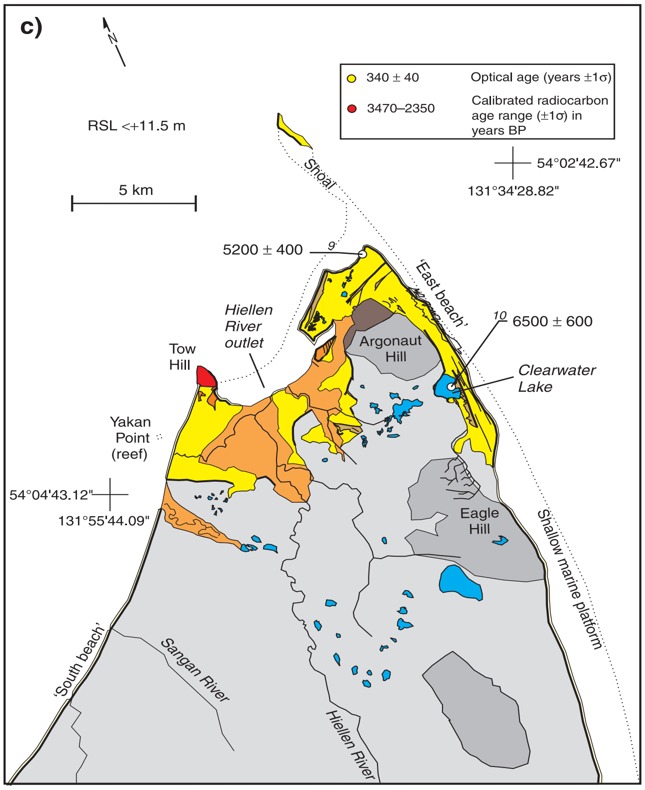

Figure 3. c) Interpreted shoreline position, surficial geology, and geomorphology for ca. 5 ka, with relevant dating control.

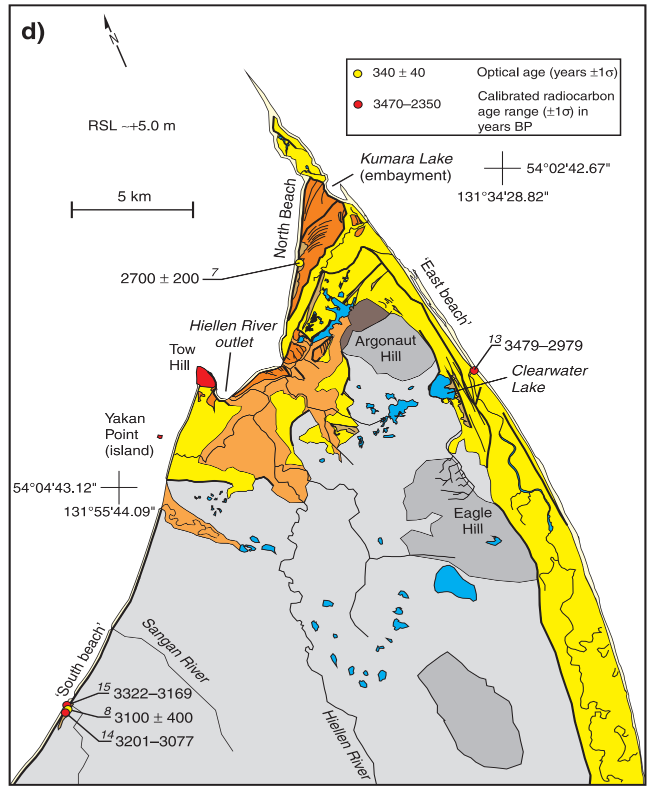

Figure 3. d) Interpreted shoreline position, surficial geology, and geomorphology for ca. 3 ka, with relevant dating control.

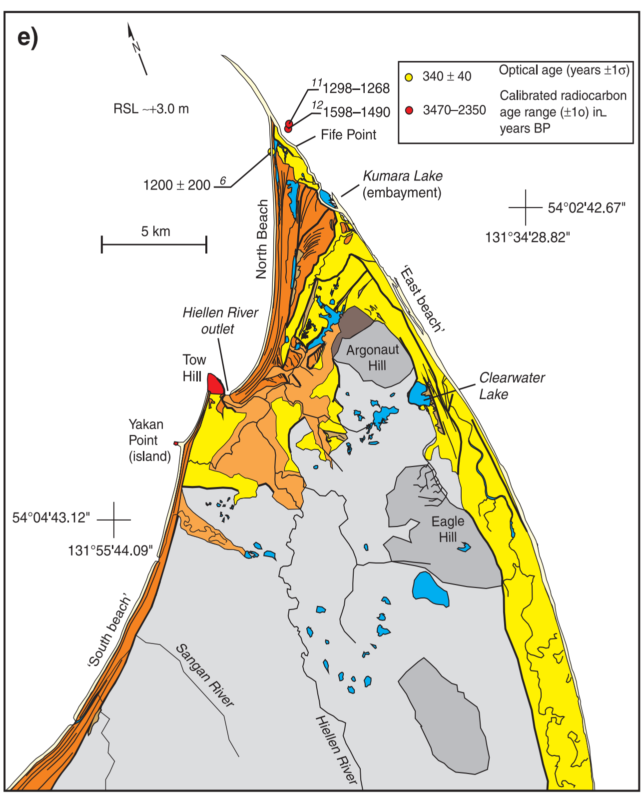

Figure 3. e) Interpreted shoreline position, surficial geology, and geomorphology for ca. 1.2 ka, with relevant dating control.

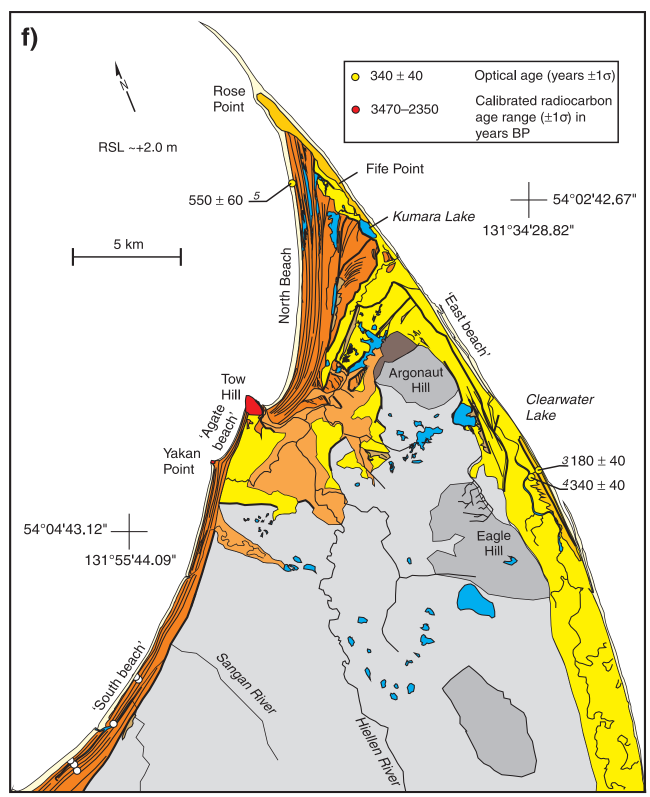

Figure 3. f) Interpreted shoreline position, surficial geology, and geomorphology for ca. 0.5 ka, with relevant dating control. RSL = relative sea level.

Wave-cut ridges are well defined at about 20 m a.m.s.l., west and southeast of Argonaut Hill (Fig. 2a, 3a). The base of these ridges, at about 18.5 m a.m.s.l., marks the Holocene marine highwater limit, below which a broad marine terrace extends across the northern Naikoon peninsula to an elevation of about 11.5 m a.m.s.l. This terrace is mantled by shallow estuaries, beaches, and foredunes, which formed during sea-level regression. Estuary sediments were deposited at river mouths in shallow tidal inlets, with beaches and foredunes forming at the outlets. A modern example of this occurs at the mouth of Hiellen River. Shore-parallel foredune ridges and stabilized parabolic dunes were also deposited on the terrace, northwest and east of Argonaut Hill (Fig. 2a, 3a).

A lower prominent wave-cut ridge occurs at an elevation of between 5.5 m a.m.s.l. and 11.5 m a.m.s.l., and is well marked by the 10 m contour (Fig. 2a, 3a). Seaward of this, a second marine terrace occurs, broadening southwards on ‘East beach’ (informal name) and fronted by a series of progradational beach ridges and foredunes to the west along North Beach. This terrace was likely formed by deposition of wave-washed sediments in the intertidal or shallow subtidal nearshore, and is extensively mantled by eolian sand.

Active sand dunes are found along most of the shoreline in the study area with older stabilized dunes occurring inland. On North Beach, ‘South beach’ (informal name), and portions of East beach active foredunes back the beach. On East beach, blowouts and transgressive parabolic dunes are widespread, extending as much 1.2 km inland and aggrading to heights of more than 20 m. Extensive eolian sand sheets, ranging from 50 cm to over 2 m thick, mantle most of the marine depositional terrace inland of East beach. In comparison, the western shoreline of Naikoon peninsula, including South beach and North Beach, comprise relict cobble-gravel beach ridges and progradational foredunes. At the northern tip of the peninsula at Rose Point, sand dunes derived from East beach have migrated over progradational ridges that parallel North Beach. Rose Spit lies north of this location, and is composed of overwash sand and gravel capped by eolian sand and, in some areas, extensive driftwood deposits.

Bluff-top dunes and sand sheets, formed by landward transport of beach sand in areas of topographically accelerated airflow, are also found to a lesser extent in the study region. Such features occur where beaches are narrow and foredunes are absent, such as atop the bluffs south of the Oeanda River and on a high ridge behind the Sangan River outlet (Fig. 3a).

Optical and radiocarbon dating

Table 3 presents the optical ages, which were all derived from eolian sand. The average analytical uncertainty in the ages at 1σ is about 12% of the reported ages, but a few (SFU-O-292, SFU-O-286) are about 15% or greater. About half of this uncertainty is derived from the uncertainty in the anomalous fading rates. Ages from two young samples were determined without fading-rate corrections. A zero-age sample (site 1, SFU-O-284) from the surface of a modern foredune blowout, exposed to light during time of sampling, returned an age of 20 ± 50 years. In comparison, the sample from site 2 (SFU-O-285) from 100 cm below a moss-covered, forested surface beyond the head of an active blowout, returned an age of -10 ± 30 years. The uncertainties in these optical ages could mask a zero-age error of up to about 30 years. The remaining optical ages range from about 180 years to 6520 years (Table 3). For samples older than about 1000 years, the zero-age error is less than 3% and is not considered significant.

Table 4 presents the radiocarbon ages determined in the study area with 1σ uncertainty. Two age determinations were made for each sample collected in marine settings (site 11, 12) to assess the reproducibility. In both cases, the differences between the initial and duplicate ages were small and, therefore, the final calibrated age ranges use the combined uncertainties. The sample from site 12 is seaweed, and the calibrated radiocarbon age was therefore determined under the assumption that it was 100% marine, which is supported by the less negative $\delta^{13}C$ values of −10.7‰ and −13.4‰ (Table 4).

For the three terrestrial samples (site 13, 14, 15), multiple age determinations were made on various subsets of the collected materials because of the potential incorporation of younger organic materials. The sample from site 14, collected at approximately 44 m a.m.s.l. at a depth of 75–80 cm in eolian sand, was used to compare to an optical age in eolian sand at 60 cm depth (site 8) from the same location. The degraded peat in the organic sample returned an age of about 3140 cal a BP (+3077, −3201 years; UCIAMS 10374) which is consistent with the optical age of 3100 ± 390 a (SFU-O-290), whereas plant stems and roots from this depth returned modern ages (UCIAMS 10147, 10533).

Samples from sites 13 and 15 were used to provide minimum limiting age estimates on relative sea level. The sample from site 13, collected at an elevation of 12.5 m a.m.s.l. returned older ages from bulk peat (UCIAMS 10528, 10142, 10150) than from the plant stems and roots (UCIAMS 10372, 10527) and therefore only the peat ages were used for an age-range estimate of 3479–2979 cal a BP. In contrast, a surface sample of charred plant fragments and peat (site 14) returned a set of ages with the charred plant fragments returning the oldest age range of 3322–3169 cal a BP (UCIAMS 10148), which was used for this age estimate.

INTERPRETATION

Late Holocene sea-level regression and shoreline evolution

Using the surficial geology and geomorphology map of the area (Fig. 3a) and age control from optical and radiocarbon dates (Table 3, 4), former sea-level positions, shoreline configurations, and surficial sediments were reconstructed for six time periods from about 9.5 ka to present (Fig. 3a–f).

ca. 9.5 ka

The Holocene marine highstand on Naikoon peninsula is well defined by wave-cut ridges with basal elevations at about +18.5 m a.m.s.l. (Fig. 3b). Assuming a tidal range similar to present, this places relative mean sea level at about 15.5 m at that time. Although materials at or above the local highstand were not dated in this study, Clague et al. (1982a) and Clague (1989) place the timing of this at between 9 ka and 10 ka (8000 ^{14}C BP and 9000 ^{14}C BP). At that time, the Rose Spit complex did not exist. Instead, Argonaut Hill was a promontory at the northern tip of Naikoon peninsula, with several bays and river outlets lying to the west (Fig. 3b).

A shallow submerged terrace may have extended seaward of the northern coast of Naikoon peninsula. Support for this interpretation comes from the consistent elevation of a preserved terrace at an elevation of 15–10 m capped by estuarine and beach sediments along this northern part of the peninsula. Given the present macrotidal range of 5–7 m, this terrace was shallowly submerged (~2–5 m depth) and likely exposed to an energetic wave and tidal regime. Barrie et al. (2005) suggested that wave energies were likely greater during the Holocene highstand than at present due to increased fetch. They further suggested that sediment supply was less than at present, as the rapid transgression had reworked and mobilized most sediment offshore. This probably explains the absence equivalent terraces along the exposed, erosional, shorelines of East beach and South beach.

A shallow offshore shoal may also have existed about 8 km north of Argonaut Hill, based on the present-day elevation of these sediments. The Hiellen River outlet (possibly occupying a former glacial spillway) and other river outlets were tidally inundated, creating small estuaries. Tow Hill was an island about 4 km offshore, and Yakan Point was a submerged rocky shoal. Clearwater Lake, south of Argonaut Hill on East beach, was a small embayment possibly partially separated from Hecate Strait by a low spit formed by the longshore drift of sediments from bluff erosion along Eagle Hill and lower bluffs to the south. The shoreline along East beach south of Eagle Hill, and along South beach from the Sangan River to Masset, were characterized by high bluffs and narrow beaches, and probably exposed to extensive wave action.

ca. 9.5–5 ka

Falling relative sea levels to below 11.5 m a.m.s.l. between 9.5 ka and 5 ka exposed shallow marine terraces and tidal inlets (Fig. 3c). Shore-parallel beach ridges and foredunes formed on the terraces as sea level regressed, whereas fluvial and estuary sediments were deposited at the outlets of several shallow rivers, most notably on the Hiellen River. At some time between 9.5 ka and 5 ka (or possibly later) a large landslide occurred along the northern face of Argonaut Hill depositing unconsolidated colluvial sediments onto the lower terrace.

On East beach, Clearwater Lake formed as spit progradation created an enclosed bay. As sea level regressed further, foredune ridges on the spit prograded seaward and parabolic dunes, formed from blowouts and fed by foredune and intertidal sediments, migrated into Clearwater Lake ca. 6.5 ± 0.6 ka (SFU-O-289). Shoreline orientation was more northerly along this stretch of East beach than it is today. The parabolic dune orientations also differ slightly from modern dunes on East beach (Fig. 3a), indicating that either strong easterly, rather than southeasterly, winds prevailed at that time either due to changing synoptic wind conditions or local topographic steering effects from Argonaut Hill. It should be noted that, unlike foredunes, parabolic dune alignments are predominantly controlled by prevailing competent winds, not shoreline orientation.

As sea level regressed, the offshore shoal to the north of Argonaut Hill emerged, forming an island north of the tip of Naikoon peninsula. This may be similar to the modern 'Rose bar' (informal name; a supratidal gravel island) that presently extends 2–3 km northeast of the tip of Rose Spit connected via a narrow, sinuous subtidal shoal. Continued northward littoral drift along East beach and some northeasterly drift along North Beach may have formed a shallow, subtidal shoal between the island and the mainland.

A distinctive and fairly contiguous wave-cut ridge incised into the marine terrace marks a period of shoreline erosion when sea level was about 8.5 m a.m.s.l., ca. 5.2 ± 0.4 ka (SFU-O-287). By that time, Tow Hill was attached to the mainland by exposure of the marine terrace and the expansion of the Hiellen River estuary, and the bedrock outcrop at Yakan Point was a small submerged reef.

ca. 5–3 ka

A drop in relative sea level to about 4.5 m a.m.s.l., exposed sandy depositional marine terraces along East beach and the northern end of Naikoon peninsula (Fig. 3d). The terrace along East beach probably aggraded due to continued erosion of bluff systems further to the south (e.g. Cape Ball) and northward littoral drift. Northern portions of this terrace are capped with eolian sand; however, it is believed that sea-level regression was fairly rapid during this time and that the marine terrace extended seaward of the mapped extent. As East beach has been dominantly erosional since ca. 3 ka (below), any evidence of dune systems on the seaward edge has been eroded. A radiocarbon age of peat, overlying marine sediments, at an elevation of about 12.0 m a.m.s.l. indicates terrestrial exposure here prior to 3479–2979 cal a BP (UCIAMS 10128, 10142, 10150).

The subtidal shoal connecting Naikoon peninsula and the island to the north became a subaerial spit platform extending about 10 km north of Argonaut Hill into Hecate Strait. On the western side of this spit, extending from the Hiellen River estuary, a depositional sink formed, favouring the development of a series of recurved spits and progradational beach ridges capped with eolian sand. Arcuate alignments of these ridges indicate northward progression of beach progradation into a cuspate embayment. This progradation was interspersed with erosion, as evidenced by wave-cut bluffs in the ridge sequence. As progradation continued, ridge alignment shifted westward, to eventually infill the cuspate embayment and form a smoothed curvilinear shoreline. Foredunes formed along the seaward margin of this beach ridge ca. 2.7 ± 0.2 ka (SFU-O-288) as sea level fell to below 4.5 m a.m.s.l. Eastward of the progradational ridges, several beach ridges formed at the outlet of the Hiellen River and other streams. Progressive aggradation of these ridges caused the outlet positions to change continually and migrate westward.

Along South beach, the offshore bedrock reef at Yakan Point emerged as an islet. Southwest of the Sangan River, eolian sand was deposited atop a 45 m high ridge ca. 3.1 ± 0.4 ka. This indicates that a sandy shoreline remained in close proximity to the base of the ridge at that time. As noted earlier, a radiocarbon date from peat at 75–80 cm depth returned an age of between 3077 cal a BP and 3201 cal a BP (UCIAMS 10374), in keeping with the optical age. Of geoarcheological interest, a stone plank-grinding tool (Fig. 4) was found within the eolian sand coincident with the optical sample. These dates indicate that the artifact was emplaced about 3100 years ago. At that time, this promontory could have been an occupation site along the northwestern shoreline of Naikoon peninsula.

Using a prograded beach width of 800 m and assuming the bluff was abandoned from the beach ca. 3100, a progradation rate of 0.3 m/a results for this section of South beach. Previous work near this location provided similar progradation rate estimates ranging from 0.3 m/a to 0.4 m/a, based on uncalibrated shell radiocarbon ages ranging from 1300 years BP to 550 years BP (Harper, 1980; Clague et al., 1982b). Modern cross-shore monitoring profiles along South beach since 1993, however, indicate increased (albeit short-term) progradation rates of about 0.6–0.7 m/a (Walker et al., 2007).

ca. 3–1.2 ka

A rapidly prograding foredune complex along North Beach between Tow Hill and the tip of Naikoon peninsula was established after ca. 3 ka (Fig. 3e) due to high onshore sediment transport via eolian activity and swash action. Aggradation of these foredunes blocked former river outlets and forced the drainage toward a single outlet of the Hiellen River adjacent to Tow Hill. By ca. 1.2 ± 0.2 ka (SFU-O-292), sea level was at about 3 m a.m.s.l. At that time, a supratidal spit, likely capped by overwash sediments and eolian sand as a result of convergent littoral transport from North Beach and East beach, probably extended beyond the peninsula — a precursor to the modern Rose Spit complex.

Figure 4. Stone plank-grinding tool found at 'Sangan ridge' (informal name) and identified by Drs. Quentin Mackie (Department of Anthropology, University of Victoria) and Daryl Fedje (Parks Canada). The stone tool was given to the Council of Haida Nations in Masset.

Near Tow Hill, a comparatively protected bay and shallow, sandy nearshore environment probably provided an abundant resource of fish, molluscs, and crustaceans, as it does today. Except for the large Hiellen River, most river and creek outlets along North Beach were blocked by the contiguous shore-parallel beach ridges and dunes. In contrast, the East beach shoreline has been dominantly erosional since ca. 3 ka as earlier features from higher sea-level stands remain preserved (e.g. Clearwater Lake dune ridges).

Similar ages of ca. 1280 cal a BP and 1550 cal a BP from a terrestrial pine cone (UCIAMS 10143, 10529) and marine seaweed (UCIAMS 10144, 10530), respectively, indicate deposition over marine clay containing marine foraminifera (A. Dallimore, pers. comm., 2006) and nearshore marine molluscs (R. Hetherington, pers. comm., 2006) at Fife Point (Fig. 3e). This suggests that terrestrial materials were eroded and deposited into the nearshore at that time.

Some time after ca. 3 ka, a shallow terrestrial basin was isolated by beach and foredune growth on East beach trapping discharge to form Kumara Lake. This is contrary to earlier interpretations by Barrie and Conway (2002), who suggested that the lake was present and transgressed by sea level rising to the highstand in the early Holocene. The feature shown in Barrie and Conway (2002, Fig. 9) as the Early Holocene highstand shoreline behind Kumara Lake is actually part of the foredune ridge dating ca. 2.7 ± 0.2 ka (SFU-O-288) that fronted North Beach at that time (discussed above, Fig. 3d), whereas the actual highstand is at least 13 m higher and skirts Argonaut Hill several kilometres to the south.

ca 1.2–0.5 ka

For the last 1200 years, the North Beach shoreline has continued to prograde (Fig. 3f) during very gradual rates of sea-level regression (Walker and Barrie, 2006). By ca. 550 ± 60 a (SFU-O-291), sea level was at about 2 m a.m.s.l. Based on optical ages from the foredunes along North Beach, progradation has occurred at an average rate of about 1.0 m/a over the last 2700 years; however, this rate has increased from about 0.7 m/a between 2700 years and 1200 years, to 1.0 m/a between 1200 years and 550 years, and to 1.6 m/a from 550 years to present (SFU-O-292, SFU-O-288, SFU-O-291). The relatively uniform spacing and size of these foredune ridges, particularly in the last 1200 years, suggests fairly consistent wind, wave, and sediment supply conditions. These progradation rates are approximately three times faster than those estimated at South beach (to the west of Tow Hill) during the same time period due to the relatively rapid infilling of the depositional sink between Tow Hill and Rose Spit. During this period of progradation, Yakan Point may have joined the mainland.

Most of the progradational ridges formed along North Beach are foredunes, rather than beach ridges proper, which require wave swash as a formative mechanism. This is an important distinction as the role of eolian processes is typically understated in the coastal geological literature and the term ‘beach ridge’ is often misused (Hesp, 1984, 2002; Otvos, 2000). Clearly, wind has played an important role in the late Holocene coastal development of Naikoon peninsula.

Along East beach, coastal erosion predominated during this time with high onshore winds and sediment supply. This would have maintained active foredunes, blowouts, and migrating parabolic dunes, which by about 340 years ago became stabilized (as discussed in following section).

At least two Haida villages existed in the area in the last 1200 years, one at the Hiellen River and one near Rose Spit. It is likely that, as North Beach and Rose Spit prograded, village sites migrated to remain close to the shoreline.

500 years to present

Figure 3a represents the full geomorphic setting of Naikoon peninsula, including recent historical changes. Along East beach, a strong wind and wave regime caused continual coastal erosion and created large foredunes and blowouts along the shoreline. Optical ages indicate that sand dunes have migrated up to 1.2 km inland in the last few hundred years (340 ± 40 years, SFU-O-283) and onshore winds have blanketed much of the area with 2 m or more of eolian sand (180 ± 40 years, SFU-O-286). Recent eolian process studies (Pearce, 2005; Anderson and Walker, 2006) have shown that high amounts of windblown sediment (up to 110 kg/m^2 over 6 months) can be transported as much as 300 m onshore during typical winter storm winds, thereby maintaining actively accreting and migrating foredune, blowout, and parabolic dune systems on East beach.

Significant recent coastal changes have also occurred due to human activity along the shorelines of Naikoon peninsula. Most apparent is the high accumulation of driftwood, originating largely from felled lumber, which, via accumulation of extra eolian sediment in the backshore, acts to fortify the beach and established foredunes between storms (Walker and Barrie, 2006).

Historical grazing, clearing of land, and vehicle traffic has also caused localized blowouts in foredunes at numerous locations along East beach from Rose Spit to the village of Tlell (~70 km south). Logging in this area was active into the 1970s. Several large trough and saucer blowouts have been maintained by decades of vehicle traffic in the foredunes and transgressive parabolic dunes near Rose Point.

DISCUSSION AND CONCLUSIONS

This study shows that there have been significant responses in coastal landscape development since the sea-level highstand at ca. 9500 years ago. Geomorphic evidence indicates a marine hihstand at about 18.5 m, marking the maximum limit of wave erosion. Assuming that the region was subjected to similar tide and storm regimes as at present, relative mean sea level can be placed at 15.5 m, similar to elevations previously documented (Clague, 1989; Fedje and Josenhans, 2000). At the time of the highstand, the Rose Spit complex did not exist and steep, bluff-dominated shorelines from Argonaut Hill to Masset suggest extensive wave-cut erosion, narrow beaches, and little onshore sediment deposition.

Falling relative sea levels between 9500 years and 5000 years ago exposed marine terraces and estuaries mantled by shore-parallel beaches and foredunes. Parabolic dunes seaward of Clearwater Lake stabilized at about 6500 years ago.

Tow Hill did not join the mainland until about 5000 years ago. Subsequently, rapid progradation of North Beach, caused by formation of a depositional sink in the resulting embayment, progressed to modern day. In particular, the past 2700 years have seen rapid, possibly accelerating, rates of beach ridge and foredune progradation. The development of these prograding shorelines and the eventual formation of the Rose Spit complex extending from Rose Point, suggest enhanced nearshore sediment transport along both North Beach and East beach and high eolian activity action during this period.

On East beach, sea-level regression was fairly rapid between 5 ka and 3 ka. During this time, the marine terrace likely extended seaward and may have hosted dunes on the seaward edge; however, as East beach has been dominantly erosional since ca. 3 ka, evidence of older dunes on this terrace has been eroded.

Along the north shore bluffs extending from the Sangan River to Masset, limited geoarcheological evidence dating to about 3100 years ago suggests that a promontory near the outlet of the Sangan River may have been an occupation site by the Haida at that time. Within the last 3000 years, beach progradation has occurred along the coast fronting the bluffs on the north shore, and Yakan Point joined the mainland within the last 1200 years.

Strong winds have played a longstanding and significant role in the evolution of this landscape for at least the last 6500 years. They continue to do so today by maintaining extensive active dune systems on both shores. It is believed that these dune systems, coupled with additional sediment stored in backshore driftwood jams, act as a protective 'buffer' of sediment against wave attack and coastal flooding (Walker and Barrie, 2006).

Recent research has shown that the impacts of increasing climatic variability events (e.g. coastal storms and surges associated with ENSO (El Niño Southern Oscillation) and PDO (Pacific Decadal Oscillation) events) and gradual sea-level rise pose increasing threats to the shorelines and communities of northeast Graham Island. In particular, over the 20th century mean sea level in Hecate Strait rose at 1.6 cm/century and extreme annual water levels, generated by large tides and storm surges, rose at 3.4 cm/century (Abeysirigunawardena and Walker, in press). This has caused ongoing erosion on East beach of 1 m/a to 3 m/a to tens of metres in extreme seasons such as the 1997–1998 El Niño event (Barrie and Conway, 1996, 2002). Although North Beach continues to prograde seaward, notable localized erosion has occurred over the past decade, particularly around river estuaries. Future sea levels could be up to 30 cm higher by 2050 (Walker et al., 2007), with more storm surges superimposed on this. These events pose immediate and increasing risks of coastal erosion and flooding and may change the rates and results of ongoing coastal geomorphic processes on northeast Graham Island in the near future.

ACKNOWLEDGMENTS

This study was undertaken within the Municipal Case Studies project of the Reducing Canada's Vulnerability to Climate Change Program, which operated from 2002 to 2006. The study was funded in part by the Climate Change Impacts and Adaptations Directorate (CCIAD) and was a component of CCIAP Project A580. Additional funding and logistical support was provided by an NSERC Discovery Grant and CFI New Opportunity Infrastructure Grant to I.J. Walker, field equipment from Technical Field Support Services–Geological Survey of Canada, and research access permits and support from BC Parks and the Council of the Haida Nation. Identification of marine foraminifera and shells was provided by A. Dallimore (GSC Sidney) and R. Hetherington (University of Victoria) respectively. Carbon dating was conducted by J. Southon (University of California, Ervine) and assistance with optical dating was provided by N. Meisel and A.M.J. Hamel. LiDAR data processing was performed by B. Arril and D. Parton (University of Victoria) and artifact identification was undertaken by D. Fedje (Parks Canada), Q. Mackie (University of Victoria), and Captain Gold (Haida historian). Valuable field assistance was also provided by J. Anderson, V. Barrie, S. Jackson, G. Manson, A. Merilees, K. Pearce, K. Tattrie, W. Zantvoort, and the Shatz family.

REFERENCES

Abeysirigunawardena, D.S. and Walker, I.J., in press. Sea level responses to climate variability and change in northern British Columbia; Atmosphere-Ocean, v. 46, no. 2.

Aitken, M.J., 1998. An Introduction to Optical Dating; Oxford University Press, Oxford, United Kingdom, 267 p.

Anderson, J.L. and Walker, I.J., 2006. Airflow and sand transport variations within a backshore-parabolic dune plain complex: NE Graham Island, British Columbia, Canada; Geomorphology, v. 77, p. 17–34. doi:10.1016/j.geomorph.2005.12.008

Barrie, J.V. and Conway, K.W., 1996. Evolution of a nearshore and coastal macrotidal sand transport system, Queen Charlotte Islands, Canada; *in* Geology of Siliciclastic Shelf Seas, (ed.) M. DeBatist and J. Jacobs; Geological Society Special Publication no. 117, London, United Kigdom p. 233–248.

Barrie, J.V. and Conway, K.W., 1999. Late Quaternary glaciation and postglacial stratigraphy of the northern Pacific margin of Canada; Quaternary Research, v. 51, p. 113–123. doi:10.1006/qres.1998.2021

Barrie, J.V. and Conway, K.W., 2002. Rapid sea level change and coastal evolution on the Pacific margin of Canada; Journal of Sedimentary Geology, v. 150, p. 171–183. doi:10.1016/S0037-0738(01)00274-3

Barrie, J.V., Conway, K.W., Josenhans, H., Clague, J.J., Mathewes, R.W., and Fedje, D.W., 2005. Late Quaternary geology of Haida Gwaii and surrounding marine areas; *in* Haida Gwaii: Human History and Environment from the Time of the Loon to the Time of the Iron People, (ed.) D.W. Fedje and R.W. Mathewes; UBC Press, Vancouver, British Columbia, p. 7–20.

Clague, J.J., 1989. Quaternary geology of the Queen Charlotte Islands; *in* The Outer Shores, (ed.) G.G.E. Scudder and N. Gessler; Queen Charlotte Islands Museum Press, Queen Charlotte City, British Columbia, p. 65–74.

Clague, J.J., Harper, J.R., Hebda, R.J., and Howes, D.E., 1982a. Late Quaternary sea levels and crustal movements, coastal British Columbia; Canadian Journal of Earth Sciences, v. 19, p. 597–618.

Clague, J.J., Mathewes, R.F., and Warner, B.G., 1982b. Late Quaternary geology of eastern Graham Island, Queen Charlotte Islands, British Columbia; Canadian Journal of Earth Sciences, v. 19, p. 1786–1795.

Dalzell, K.E., 1968. The Queen Charlotte Islands 1774–1966; Volume 1; C.M. Adam, Terrace, British Columbia, 340 p.

Dolan, A.H. and Walker, I.J., 2006. Understanding vulnerability of coastal communities to climate change related risks; Journal of Coastal Research, (Special Issue) 39, p. 1317–1324.

Fedje, D.W. and Josenhans, H.W., 2000. Drowned forests and archaeology on the continental shelf of British Columbia, Canada; Geology, v. 28, p. 99–102. doi:10.1130/0091-7613(2000)28<99:DFAAOT>2.0.CO;2

Fedje, D.W. and Mackie, Q., 2005. Overview of cultural history; *in* Haida Gwaii: Human History and Environment from the Time of the Loon to the Time of the Iron People, (ed.) D.W. Fedje and R.W. Mathewes; UBC Press, Vancouver, British Columbia, p. 154–162.

Fedje, D.W., Mackie, A.P., McSorran, J.B., and Wilson, B., 1996. Early period archaeology in Gwaii Haanas: results of the 1993 field program; *in* Early Human Occupation of British Columbia, (ed.) R.L. Carlsen and L. Palla-Bona; University of British Columbia Press, Vancouver, Canada, p. 133–151.

Harper, J.R., 1980. Coastal processes on Graham Island, Queen Charlotte Islands, British Columbia; Current Research, Part A; Geological Survey of Canada, Paper, 80–1A, p. 13–18.

Hesp, P.A., 1984. The formation of sand “beach ridges” and foredunes; Search, v. 15, no. 9–10, p. 289–291.

Hesp, P.A., 2002. Foredunes and blowouts: initiation, geomorphology and dynamics; Geomorphology, v. 48, p. 245–268. doi:10.1016/S0169-555X(02)00184-8

Hetherington, R., Barrie, J.V., Reid, R.G.B., MacLeod, R., Smith, D.J., James, T.S., and Kung, R., 2003. Late Pleistocene coastal paleogeography of the Queen Charlotte Islands, British Columbia, Canada, and its implications for terrestrial biogeography and early postglacial human occupation; Canadian Journal of Earth Sciences, v. 40, p. 1755–1766. doi:10.1139/e03-071

Huntley, D.J. and Lamothe, M., 2001. Ubiquity of anomalous fading in K-feldspars, and the measurement and correction for it in optical dating; Canadian Journal of Earth Sciences, v. 38, p. 1093–1106. doi:10.1139/cjes-38-7-1093

Huntley, D.J. and Lian, O.B., 1999. Using optical dating to determine when a mineral grain was last exposed to sunlight; *in* Holocene Climate and Environmental Change in the Palliser Triangle: a Geoscientific Context for Evaluating the Impacts of Climate Change in the Southern Canadian Prairies, (ed.) D.S. Lemmen and R.E. Vance; Geological Survey of Canada, Bulletin 534, p. 211–222.

Intergovernmental Panel on Climate Change, 2007. Climate Change 2007: The Physical Science Basis; Summary for Policymakers, IPCC WGI Fourth Assessment Report, 18 p.

Josenhans, H.W., Fedje, D.W., Conway, K.W., and Barrie, J.V., 1995. Post glacial sea levels on the western Canadian continental shelf: evidence for rapid change, extensive subaerial exposure, and early human habitation; Marine Geology, v. 125, p. 73–95. doi:10.1016/0025-3227(95)00024-S

Josenhans, H., Fedje, D., Pienitz, R., and Southon, J., 1997. Early humans and rapidly changing Holocene sea levels in the Queen Charlotte Islands–Hecate Strait, British Columbia, Canada; Science, v. 277, p. 71–74. doi:10.1126/science.277.5322.71

Lian, O.B. and Huntley, D.J., 2001. Luminescence dating; *in* Tracking Environmental Change Using Lake Sediments. Volume 1: Basin Analysis, Coring, and Chronological Techniques, (ed.) W.M. Last and J.P. Smol; Kluwer Academic Publishers, Dordrecht, the Netherlands, p. 261–282.

Lian, O.B., Huntley, D.J., and Wolfe, S.A., 2002. Optical dating of eolian dune sand from the Canadian prairies; Géographie physique et Quaternaire, v. 56, p. 191–202.

Mackie, Q. and Acheson, S., 2005. The Graham Tradition; *in* Haida Gwaii: Human History and Environment from the Time of the Loon to the Time of the Iron People, (ed.) D.W. Fedje and R.W. Mathewes; UBC Press, Vancouver, British Columbia, p. 274–302.

Ommer, R.E., 2007. Coasts Under Stress: Restructuring and Social-Ecological Health; McGill-Queen’s University Press, Montreal, Quebec, 624 p.

Otvos, E.G., 2000. Beach ridges - definitions and significance; Geomorphology, v. 32, p. 83–108. doi:10.1016/S0169-555X(99)00075-6

Pearce, K.I., 2005. Aeolian geomorphology of NE Graham Island, Haida Gwaii (Queen Charlotte Islands), British Columbia; M.Sc. thesis, University of Victoria, Victoria, British Columbia, 200 p.

Reimer, P.J., Baillie, M.G.L., Bard, E., Bayliss, A., Beck, J.W., Bertrand, C.J.H., Blackwell, P.G., Buck, C.E., Burr, G.S., Cutler, K.B., Damon, P.E., Edwards, R.L., Fairbanks, R.G., Friedrich, M., Guilderson, T.P., Hogg, A.G., Hughen, K.A., Kromer, B., McCormac, F.G., Manning, S.W., Ramsey, C.B., Reimer, R.W., Remmele, S., Southon, J.R., Stuiver, M., Talamo, S., Taylor, F.W., van der Plicht, J., and Weyhenmeyer, C.E., 2004. IntCal04 terrestrial radiocarbon age calibration, 26–0 ka BP; Radiocarbon, v. 46, p. 1029–1058.

Severs, P.D., 1975. Recent research into the prehistory of the Queen Charlotte Islands; The Midden, v. 7, p. 15–17.

Shaw, J., Taylor, R.B., Forbes, D.L., Ruz, M.-H., and Solomon, S., 1998. Sensitivity of the coast of Canada to sea level rise; Geological Survey of Canada, Bulletin 505, p. 79.

Stuiver, M., Reimer, P.J., and Reimer, R., 2005. CALIB 5.0.1 (www program and documentation); (http://www.calib.qub.ac.uk/calib/; accessed 2008-03)

Sutherland Brown, A., 1968. Geology of the Queen Charlotte Islands, British Columbia; British Columbia Department of Mines and Petroleum Resources, Bulletin 54, 220 p.

Walker, I.J. and Barrie, J.V., 2006. Geomorphology and sea-level rise on one of Canada's most 'sensitive' coasts: Northeast Graham Island, British Columbia; Journal of Coastal Research, v. 31, p. 220–226.

Walker, I.J. and Sydneysmith, R., 2008. British Columbia; *in* From Impacts to Adaptation: Canada in a Changing Climate 2007, (ed.) D.S. Lemmen, F.J. Warren, J., Lacroix, and E. Bush; Government of Canada, Ottawa, Ontario, p. 329–386.

Walker, I.J., Barrie, J.V., Dolan, H., Gedalof, Z., Manson, G., Smith, D., and Wolfe, S.A., 2007. Coastal vulnerability to climate change and sea-level rise, Northeast Graham Island, Haida Gwaii (Queen Charlotte Islands), British Columbia; CCIAP A580 Final Report, Climate Change Impacts & Adaptation Directorate, NRCan, Ottawa, 253 p.

Warner, B.G., Mathewes, R.W., and Clague, J.J., 1982. Ice-free conditions on the Queen Charlotte Islands, British Columbia, at the height of Late Wisconsin Glaciation; Science, v. 218, p. 675–677. PubMed doi:10.1126/science.218.4573.675

Wilson, J. and Harris, H., 2005. Tllsda Xaaydas K'aaygang.nga: long, long ago ancient stories; *in* Haida Gwaii: Human History and Environment from the Time of the Loon to the Time of the Iron People, (ed.) D.W. Fedje and R.W. Mathewes; UBC Press, Vancouver, British Columbia, p. 121–139.

Wintle, A.G., 1997. Luminiscence dating: laboratory procedures and protocols; Radiation Measurements, v. 27, p. 769–817. doi:10.1016/S1350-4487(97)00220-5

Wolfe, S.A., Huntley, D.J., and Lian, O.B., 2002. Holocene eolian activity in south-central Saskatchewan and the southern Canadian prairies; Géographie physique et Quaternaire, v. 56, p. 215–227.

Wolfe, S.A., Huntley, D.J., and Ollerhead, J., 2004. Relict Late Wisconsinan dune fields of the northern Great Plains, Canada; Géographie physique et Quaternaire, v. 58, p. 323–336.

Geological Survey of Canada Project J36.